



# Effect of roxadustat on serum metabolome and lipidome in patients with end-stage renal disease and erythropoiesis-stimulating agent resistance

Lichao Wang<sup>1,2#</sup>, Yulin Wu<sup>3,4#</sup>, Yongjiang Li<sup>5</sup>, Lianlian You<sup>3,4</sup>, Xinyu Liu<sup>1</sup>, Zhihong Wang<sup>3,4</sup>, Jia Xiao<sup>3,4</sup>, Shuang Zhang<sup>3,4</sup>, Tianrun Xu<sup>1,2</sup>, Xiaolin Wang<sup>1</sup>, Qi Li<sup>1</sup>, Chunxiu Hu<sup>1</sup>, Guowang Xu<sup>1</sup>, Shuxin Liu<sup>3,4</sup>

<sup>1</sup>CAS Key Laboratory of Separation Sciences for Analytical Chemistry, Dalian Institute of Chemical Physics, Chinese Academy of Sciences, Dalian, China; <sup>2</sup>University of Chinese Academy of Sciences, Beijing, China; <sup>3</sup>Department of Nephrology, Dalian Municipal Central Hospital, Dalian, China; <sup>4</sup>Dalian Key Laboratory of Intelligent Blood Purification, Dalian Municipal Central Hospital, Dalian, China; <sup>5</sup>School of Optoelectronic Engineering and Instrumentation Science, Dalian University of Technology, Dalian, China

**Contributions:** (I) Conception and design: G Xu, S Liu, C Hu; (II) Administrative support: None; (III) Provision of study materials or patients: Y Wu, L You, Z Wang, J Xiao, S Zhang, T Xu, X Wang, Q Li; (IV) Collection and assembly of data: L Wang, Y Wu, L You, Z Wang, J Xiao, S Zhang, T Xu, X Wang, Q Li; (V) Data analysis and interpretation: L Wang, Y Wu, L You, YJ Li, Z Wang, X Liu; (VI) Manuscript writing: All authors; (VII) Final approval of manuscript: All authors.

<sup>#</sup>These authors contributed equally to this work and should be considered as co-first authors.

**Correspondence to:** Chunxiu Hu, PhD; Guowang Xu, PhD. CAS Key Laboratory of Separation Sciences for Analytical Chemistry, Dalian Institute of Chemical Physics, Chinese Academy of Sciences, Dalian, China. Email: hucx@dicp.ac.cn; xugw@dicp.ac.cn; Shuxin Liu, MD, PhD. Department of Nephrology, Dalian Municipal Central Hospital, No. 826, Xinan Road, Dalian 116033, China. Email: root8848@sina.com.

**Background:** Roxadustat is a newly marketed hypoxia-inducible factor prolyl hydroxylase inhibitor used to treat anemia in patients with end-stage renal disease (ESRD). While clinical trials have demonstrated the therapeutic effects of roxadustat in patients with ESRD who are resistant to erythropoiesis-stimulating agents (ESAs), its metabolic effects are still unclear.

**Methods:** Thirty-two individuals with ESRD and ESA resistance from the Blood Purification Center of Dalian Municipal Central Hospital were included. A total of 96 fasting serum samples were obtained from participants before treatment with roxadustat, and after treatment for 15 and 30 days. Ultra-high performance liquid chromatography-mass spectrometry-based metabolomics and lipidomics strategies were applied to investigate the effects of roxadustat on serum metabolism.

**Results:** A total of 255 metabolites and 444 lipid molecular species were detected and quantified. Sphingolipids and phospholipids decreased significantly during treatment, possibly associated with changes in phospholipid and ceramide metabolism. Bile acid levels decreased and cholic acid/chenodeoxycholic acid increased, indicating changes in gut microbiota and bile acid metabolism. Amino acids also changed during the process of treatment.

**Conclusions:** The present study showed sphingolipids, phospholipids, and bile acids were significantly altered, which may be associated with a changed metabolism caused by roxadustat. This approach provided a powerful tool for exploring the mechanisms of ESA resistance in ESRD patients and may represent a promising strategy for elucidating the complex therapeutic mechanisms of other drugs.

**Keywords:** Anemia; erythropoiesis-stimulating agent resistance; lipidomics; metabolomics; ultra-high performance liquid chromatography-mass spectrometry

Submitted Aug 16, 2022. Accepted for publication Oct 09, 2022.

doi: 10.21037/atm-22-4451

View this article at: <https://dx.doi.org/10.21037/atm-22-4451>

## Introduction

Renal anemia is a common complication in patients with chronic kidney disease (CKD), especially in end-stage renal disease (ESRD) (1). The incidence of anemia increases with the progress of CKD, and investigations have shown an incidence in ESRD of >90% (2), which further increases the risk of cardiovascular events and death (3,4). While traditional treatment for renal anemia includes erythropoietin and iron supplements (5), around 5–10% of patients show significant resistance to erythropoiesis-stimulating agents (ESAs) (6), mainly as a result of iron deficiency and inflammation (7,8). Roxadustat is a hypoxia-inducible factor prolyl hydroxylase inhibitor (HIF-PHI), which regulates erythropoiesis via the HIF pathway. It has been proven to be effective in the treatment of renal anemia (9), especially in patients with ESA resistance, and can effectively improve iron metabolism and reduce inflammation (7,9). However, the metabolomic changes occurring during roxadustat treatment remain unclear.

Metabolomics and lipidomics are powerful tools for identifying and quantifying small molecular metabolites within a biological system under different pathophysiological conditions. They can measure subtle metabolic alterations in a cell or organism in a specific physiologic state and help detect the complex metabolic changes occurring during the development of disease. These methods have recently been widely used in various aspects of disease research, including early detection (10,11), drug treatment (12–14), and mechanisms (15,16). Metabolomics was used to investigate the effect of agar oligosaccharide-iron on metabolism in rats with iron-deficiency anemia by comparing normal, anemia model, and agar oligosaccharide-iron complex supplementation groups (17), and the results indicated 17 metabolites and 8 lipids were significantly changed in the serum and liver of the treated rats. These molecules might be associated with processes including the biosynthesis of saturated and unsaturated fatty acids, sphingolipid metabolism, and glycerophospholipid metabolism. In another study, researchers observed significantly decreased levels of volatile organic compounds, such as short-chain fatty acids and esters, and increased aldehydes in the feces of patients with iron-deficiency anemia after oral iron supplementation (18). Additionally, oral and intravenous iron-replacement therapy affected the fecal metabolome and bacterial communities in anemic patients with inflammatory bowel disease, leading to lower levels of cholesterol and bile acid derivatives (14).

In this study, we used metabolomics and lipidomics technologies to explore changes in lipids and metabolites in ESRD patients with ESA resistance treated with roxadustat. The study aimed to elucidate the specific effects of roxadustat on the global lipidome and metabolome, and their potential roles in its mechanism of action. To achieve this aim, we obtained 96 serum samples from 32 ESRD patients with ESA resistance before and after roxadustat treatment for 15 and 30 days and subjected them to metabolomics and lipidomics analyses. We present the following article in accordance with the MDAR reporting checklist (available at <https://atm.amegroups.com/article/view/10.21037/atm-22-4451/rc>).

## Methods

### *Study population*

This self-controlled study enrolled 32 patients with renal anemia who were undergoing hemodialysis in the Blood Purification Center of Dalian Municipal Central Hospital Affiliated of Dalian Medical University (Dalian, China). The inclusion criteria were age  $\geq 18$  years, ESA resistance, stable hemodialysis three times weekly for >12 weeks, and availability of complete medical records. The exclusion criteria were patients with tumors, those using antibiotics, immunosuppressants, or glucocorticoids in the past 3 months, and patients unable to cooperate actively with medical staff for treatment. ESA resistance was defined as the failure to attain the target hemoglobin concentration ( $< 11$  g/dL) while receiving >300 IU/kg/week (20,000 IU/week) of erythropoietin or 1.5 mg/kg of darbepoetin- $\alpha$  (100 mg/week) over a 3-month period, or a continued need for high dosages to maintain the target (19).

### *Reagents*

High-performance liquid chromatography-grade acetonitrile, methanol, chloroform, and isopropanol were purchased from Merck (Darmstadt, Germany), formic acid was purchased from J&K Scientific (Beijing, China), and methyl tert-butyl ether (MTBE) and ammonium acetate were obtained from Sigma-Aldrich (St. Louis, MO, USA). Ultrapure water was prepared using the Milli-Q system (Millipore, Billerica, MA, USA).

Carnitine (Car) C2:0-d3, Car C10:0-d3, Car C16:0-d3, phenylalanine-d5 (Phe-d5), tryptophan-d5 (Trp-d5),

cholic acid-d4 (CA-d4), and chenodeoxycholic acid-d4 (CDCA-d4) were purchased from Sigma-Aldrich and used as the internal standards (IS) for metabolomic profiling. Phosphatidylcholine 19:0/19:0 (PC 19:0/19:0), phosphatidylethanolamine 15:0/15:0 (PE 15:0/15:0), sphingomyelin d18:1/12:0 (SM d18:1/12:0), triacylglycerol 15:0/15:0/15:0 (TAG 15:0/15:0/15:0), ceramide d18:1/17:0 (Cer d18:1/17:0), lysophosphatidylcholine 19:0 (LPC 19:0), and free-fatty acids (FFAs) C16:0-d3 and C18:0-d3 were obtained from Avanti Polar Lipids (Alabaster, AL, USA) and used as IS for lipidomic profiling. For metabolomics study, Car C2:0-d3 (0.1 µg/mL), Car C10:0-d3 (0.1 µg/mL), Car C16:0-d3 (0.1 µg/mL), Phe-d5 (2.0 µg/mL), Trp-d5 (2.0 µg/mL), FFA 16:0-d3 (2.0 µg/mL), FFA 18:0-d3 (2.0 µg/mL), LPC 19:0 (1.0 µg/mL), SM d18:1/12:0 (0.1 µg/mL), CA-d4 (1.0 µg/mL), and CDCA-d4 (1.0 µg/mL) were dissolved in methanol as an extraction solvent. For lipidomics study, PC 19:0/19:0 (0.9 µg/mL), PE 15:0/15:0 (0.8 µg/mL), LPC 19:0 (0.7 µg/mL), SM d18:1/12:0 (0.8 µg/mL), TAG 15:0/15:0/15:0 (0.6 µg/mL), Cer d18:1/17:0 (0.8 µg/mL), FFA 16:0-d3 (0.6 µg/mL), and FFA 18:0-d3 (0.2 µg/mL) were dissolved in methanol as an extraction solvent.

### **Sample collection**

Fasting serum samples were obtained from the 32 patients who were all suffering from anemia and were medicated with roxadustat (FibroGen, Inc.). All patients were initially dosed thrice weekly, based on their body weight (45 to <60 kg, 100 mg; ≥60 kg, 120 mg), and were taking conventional antihypertensive and phosphate binder agents, although none were receiving intravenous iron. No treatment-related adverse effects were observed among the patients. The samples were collected at three time points: Before roxadustat treatment, and after 15 and 30 days of treatment. The study was approved by the Institutional Medical Ethics Committee of Dalian Municipal Central Hospital (No. 2020-044-08), and all participants provided written informed consent after reviewing the study plan. The study was conducted in accordance with the Declaration of Helsinki (as revised in 2013). All serum samples were stored at -80 °C prior to sample preparation.

### **Sample preparation**

#### **Metabolomics**

Fifty microliters of serum was mixed with 200 µL ice-cold

methanol containing IS in a 1.5 mL Eppendorf tube. The mixture was vortexed for 30 s for protein precipitation and metabolite extraction, placed on ice for 10 min, then centrifuged at 14,000 ×g and 4 °C for 15 min. A total of 180 µL of supernatant was collected then transferred to a new 1.5 mL Eppendorf tube for vacuum concentration at 4 °C using a CentriVap Centrifugal Vacuum Concentrator (Labconco, MO, USA). The dried residue was reconstituted in 80 µL water/acetonitrile 4:1 (v/v) and the solution was further centrifuged at 14,000 ×g and 4 °C for 15 min, and the supernatant was used for liquid chromatography-mass spectrometry (LC-MS) metabolite analysis.

#### **Lipidomics**

Forty microliters of serum was mixed with 300 µL ice-cold methanol containing IS in a 2.0 mL Eppendorf tube. After thorough vortexing for 30 s, 1 mL MTBE was added to the mixture and vibrated for 1 h at room temperature for thorough extraction of the lipids, and 250 µL ultrapure water was added to the mixture. After vortexing for 30 s and placing on ice for 10 min, the mixture was centrifuged at 14,000 ×g and 4 °C for 10 min. A total of 400 µL supernatant was then collected and transferred to a new 1.5 mL Eppendorf tube for vacuum concentration at 4 °C using a CentriVap Centrifugal Vacuum Concentrator. The dried residue was then reconstituted with 30 µL chloroform/methanol 2:1 (v/v) and 60 µL acetonitrile/isopropanol/water 13:6:1 (v/v/v), before the solution was centrifuged at 14,000 ×g and 4 °C for 15 min, and the supernatant used for LC-MS lipidomics analysis.

### **LC-MS-based metabolomics and lipidomics analyses**

#### **Metabolomics**

Metabolomic profiling was performed using an ultra-high performance liquid chromatography (UPLC) system (Waters, Milford, MA, USA) coupled to a quadrupole time-of-flight mass spectrometer (TripleTOF 5600+; AB SCIEX, Framingham, MA, USA). In positive ionization mode, metabolite separation was achieved using a BEH C8 column (2.1×50 mm, 1.7 µm; Waters) at a column temperature of 60 °C and flow rate of 0.4 mL/min. Ultrapure water with 0.1% formic acid (v/v) was used as mobile phase A and acetonitrile containing 0.1% formic acid (v/v) as mobile phase B. The elution gradient started with 5% B for 0.5 min and increased linearly to 40% B at 2 min, followed by a linear increase to 100% B at 8 min, maintained at 100% B for 2 min. The elution gradient finally returned to 5%

**Table 1** Baseline clinical characteristics of study subjects

Clinical characteristics	Value
Gender (male/female)	20/12
Age (years)	53.78±16.02
Hemodialysis (months)	49.78±48.68
Albumin (g/L)	38.86±5.11
Calcium ion (mmol/L)	2.17±0.17
Phosphorus (mmol/L)	2.01±0.66
Parathyroid hormone (pg/mL)	452.54±336.46
Hemoglobin (g/L)	85.11±10.34
Hemoglobin after 15 days of treatment (g/L)	98.42±11.92
Hemoglobin after 30 days of treatment (g/L)	101.72±14.02

The data are present with mean ± standard deviation.

B in 0.1 min, followed by equilibration with 5% B in the next 1.9 min. The scan range of precursor ion was set at 50–1,200 m/z in full-scan mode. The curtain gas was 0.241 MPa, spray voltage floating (SVF) 5,500 V, declustering potential (DP) 100 V, collision energy (CE) 30 V, and gas 1 and gas 2 were both 0.276 MPa. In negative ionization mode, metabolite separation was achieved using an HSS T3 column (2.1×50 mm, 1.8 μm; Waters) at 60 °C, and the flow rate was set at 0.4 mL/min. Ultrapure water with 6.5 mM ammonium bicarbonate was used as mobile phase A and mobile phase B was 95% methanol/water (v/v) containing 6.5 mM ammonium bicarbonate. The elution gradient conditions were 2% B for 0.5 min, increased linearly to 40% B at 2 min, followed by a linear increase to 100% B at 8 min, and maintained at 100% B for 2 min. The elution gradient then returned to 2% B in 0.1 min, followed by equilibration with 2% B in the next 1.9 min. The scan range of precursor ion was set at 50–1,200 m/z in full-scan mode, the curtain gas was 0.241 MPa, SVF was –4,500 V, DP was –100 V, CE was –30 V, and gas 1 and 2 were both 0.276 MPa.

### Lipidomics

Lipidomics profiling was performed using a UPLC system (Waters) coupled to a Q Exactive HF mass spectrometer (Thermo Scientific, Rockford, IL, USA). The lipids were separated using a BEH C8 column (2.1×100 mm, 1.7 μm; Waters) at 60 °C and the flow rate was set at 0.3 mL/min. The mobile phase A was 60% acetonitrile/water (v/v) with 10 mM ammonium acetate and phase B was 90%

isopropanol/acetonitrile (v/v) containing 10 mM ammonium acetate. The elution gradient conditions were 50% B for 1.5 min, linearly increased to 85% B at 9 min and further linearly increased to 100% B in 0.1 min, and maintained at 100% B for 1.9 min. The elution gradient then returned to 50% B in 0.1 min, followed by equilibration with 50% B in the next 1.9 min. The scan range of precursor ion was set at 300–1,100 m/z (ESI+) and 160–1,600 m/z (ESI–) in full-scan mode, while the sheath gas flow rate was 45 arb and aux gas flow rate was 10 arb. The spray voltages were 3.5 kV (ESI+) and –3.0 kV (ESI–), the capillary temperature was 320 °C, the aux gas heater temperature was 350 °C, and the resolution was set at 140,000 (full width at half maximum at 200 m/z).

### Data processing and statistical analysis

The metabolomics data were quantified using MultiQuant 3.0 software (AB SCIEX) and the lipidomics data were quantified using TraceFinder software (Thermo Scientific). The peak area of each analyte was normalized by that of the corresponding IS. The relative standard deviation (RSD) of each detected metabolite and lipid in quality control samples (QCs) was calculated, and those with an RSD <30% were kept for further statistical analysis.

A principal component analysis (PCA) model and molecular trajectory plots were established using SIMCA-P software (Umetrics, Umeå, Sweden). The nonparametric paired test and false discovery rate (FDR) test-based Benjamini and Hochberg method were applied to select metabolites and lipids that were significantly changed ( $P < 0.05$  and  $FDR < 0.05$ ) between groups. A heat-map was created using the open-source software MultiExperiment Viewer (MeV, version 4.9.0).

## Results

### Clinical characteristics of studied subjects

The clinical characteristics of the participants are listed in *Table 1*. Hemoglobin, as an indicator of anemia, increased significantly from 85.11±10.34 to 98.42±11.92 g/L after 15 days of treatment, and further increased to 101.72±14.02 g/L after 30 days of treatment.

### Data quality evaluation and global metabolic changes between groups

A total of 255 metabolites and 444 lipids were identified in

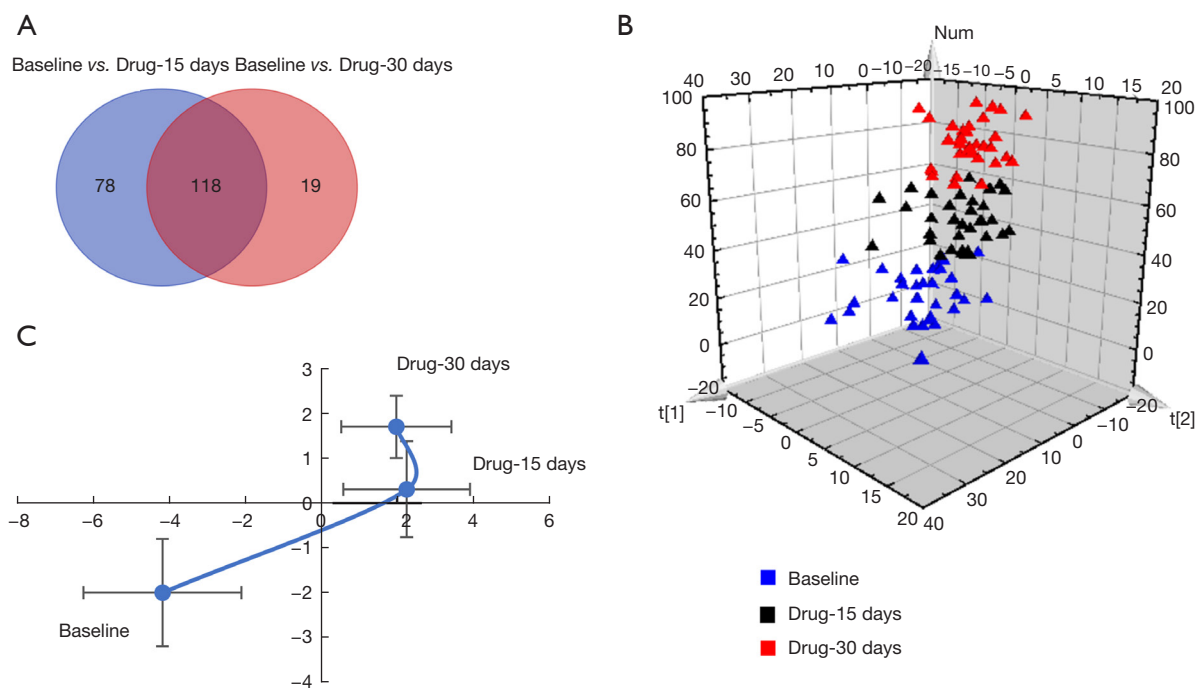


**Figure 1** Discriminant analysis of the three groups. (A) Venn diagram displaying differential metabolites after 15 and 30 days of drug treatment, compared with baseline; (B) principal component analysis scores plot; (C) molecular trajectory plots.

this study, and before statistical analysis, the qualities of the detected metabolome and lipidome data were evaluated. The distribution of the RSDs of the metabolites and lipids in 11 quality control samples are shown in Figure S1, which reveals 99.6% of 255 metabolites had an RSD <30%, which accounted for about 99.9% of the total areas of all detected metabolites (Figure S1A). Similarly, 98.9% lipids possessed an RSD <30%, accounting for 99.7% of the total areas (Figure S1B). As these results indicated the acquired metabolomics and lipidomics data were stable and adequate for exploration of the biological system, to acquire an unbiased outcome, only compounds with an RSD <30% were used for further statistical analysis.

The global metabolic changes among groups were analyzed by nonparametric paired tests. In total, 215 compounds (seven metabolites and 208 lipids) showed significantly differential levels among the groups (Figure 1A), including 196 significantly changed compounds between baseline and 15 days, and 137 significantly changed compounds between baseline and 30 days. The two drug-treatment groups had 118 common differential compounds compared with the baseline group, and we applied a pattern recognition technique to show the differences among the

three groups. The plot of the PCA model demonstrates the levels of metabolites and lipids were obviously affected by roxadustat treatment (Figure 1B). Additionally, metabolic trajectory analysis was performed to depict the time-dependent metabolic behaviors resulting from roxadustat intervention, and the plots (Figure 1C) revealed apparent alterations in metabolism after drug treatment for 15 days, which were less conspicuous between drug treatment for 15 and 30 days. We speculate these changes in metabolism might be correlated with the improved clinical hemoglobin levels.

#### *Influence of roxadustat on serum lipidomics in ESRD patients with ESA resistance*

To clarify the effect of drug intervention on lipids, we investigated the individual and total lipid contents of each lipid (sub)class in the three groups, and changes in individual lipids between baseline and the drug-treatment groups were illustrated by volcano plots. Alteration in lipids between baseline and 15 days revealed smaller P values for Cers, PCs, and PEs, and bigger fold changes for TGs ( $P < 0.05$  and  $FDR < 0.05$ ) (Figure 2A). Similarly, Cers, PCs,

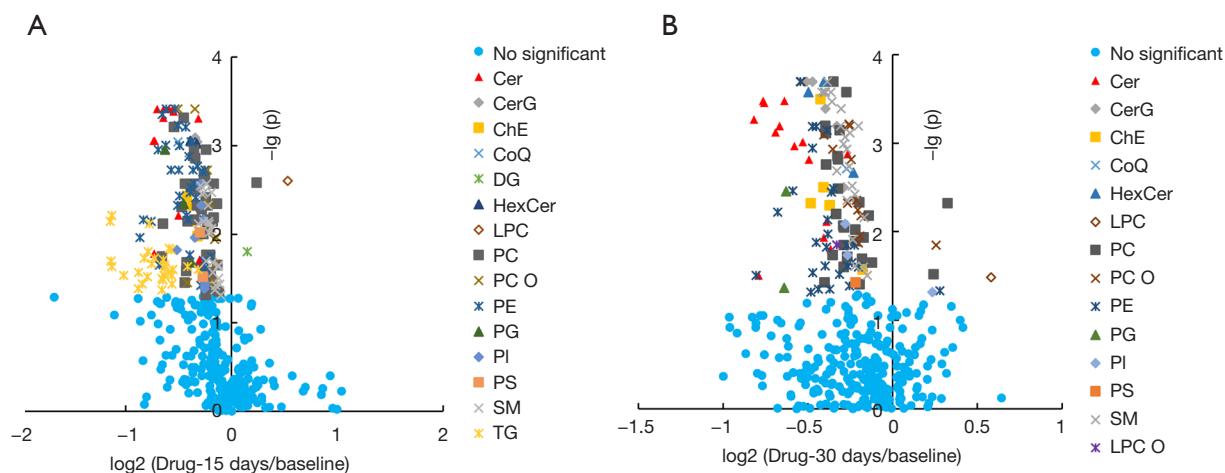


**Figure 2** Volcano plot of lipids in drug-treatment groups compared with baseline. (A) Drug-15 days *vs.* baseline; (B) drug-30 days *vs.* baseline. Red triangles: significantly changed lipids ( $P < 0.05$  and  $FDR < 0.05$ ); blue dots: lipids with no significant change. P values and FDRs of lipids calculated by nonparametric paired tests in Matlab. FDR, false discovery rate; Cer, ceramide; CerG, galactosylceramide; ChE, cholesteryl ester; CoQ, coenzyme Q; DG, diacylglycerol; HexCer, hexosylceramide; LPC, lysophosphatidylcholine; PC, phosphatidylcholine; PC O, ether bond-containing PC; PE, phosphatidylethanolamine; PG, phosphatidylglycerol; PI, phosphatidylinositol; PS, phosphatidylserine; SM, sphingomyelin; TG, triacylglycerol; LPC O, ether bond-containing lysophosphatidylcholine.

and PEs still had smaller P values after 30 days of drug treatment compared with the baseline group (Figure 2B). However, TGs showed no significant changes and had recovered to the baseline level after 30 days of treatment.

Nonparametric paired tests of the total contents of each lipid (sub)class indicated Cers, CerGs, cholesterol ester, hexosylceramide (HexCers), PCs, PC-Os, PEs, phosphatidylglycerol (PGs), phosphatidylinositols (PIs), phosphatidylserines (PSs), and sphingomyelins (SMs) were all significantly decreased after drug treatment for either 15 or 30 days (Figure 3A). Moreover, PCs, PEs, PIs, and PSs increased slightly between 15 and 30 days. For example, the 15-day/baseline ratio of PEs was 0.79 ( $P < 0.0001$  and  $FDR = 0.0004$ ), while the 30-day/baseline ratio was 0.81 ( $P = 0.0019$  and  $FDR = 0.0076$ ). However, the difference in PEs between 15 and 30 days was not significant ( $FC_{\text{drug-15 days/drug-30 days}} = 0.97$ ,  $P = 0.1782$  and  $FDR = 0.5160$ ). Other lipid (sub)classes further decreased between 15 and 30 days, but the differences were also not significant. The characteristics of lipids during lipid metabolism were also investigated, and the lipid pathways are shown in Figure 3B, which shows that the levels of phospholipids, ceramides, and sphingomyelins were obviously reduced. These changes in lipid metabolism might be closely related to the therapeutic effect of roxadustat in patients with anemia.

#### *Influence of roxadustat on serum metabolomics in ESRD patients with ESA resistance*

We also defined significantly changed metabolites in the drug-treatment groups versus baseline by nonparametric paired tests with FDRs, and CDCA, ursodeoxycholic acid (UDCA), and thyroxine showed decreasing trends after drug treatment for 15 days and significant decreases after 30 days compared with baseline (Figure 4). In contrast, valine, homoserine, betaine, and dimethylglycine displayed either increasing trends or significant increases after drug treatment for 15 days, and all were significantly increased after drug treatment for 30 days.

Notably, the class of metabolites and ratio of two metabolites can also reveal physiological changes in biological systems. Bile acids are known to be highly associated with gut microbiota, which have important effects on maintaining health. By comparing the ratios of two specific bile acids and the sum of bile acid subclasses, we observed CA/CDCA and GLCA/CDCA significantly increased after drug treatment for 30 days, while DCA/TCA, GDCA/GCA, GDCA/TCA, UDCA/TCDC, GUDCA/TCDC, and unconjugated bile acids were significantly decreased (Figure 5A). However, neither of these ratios nor the unconjugated bile acids showed any significant difference after 15 days of drug treatment.

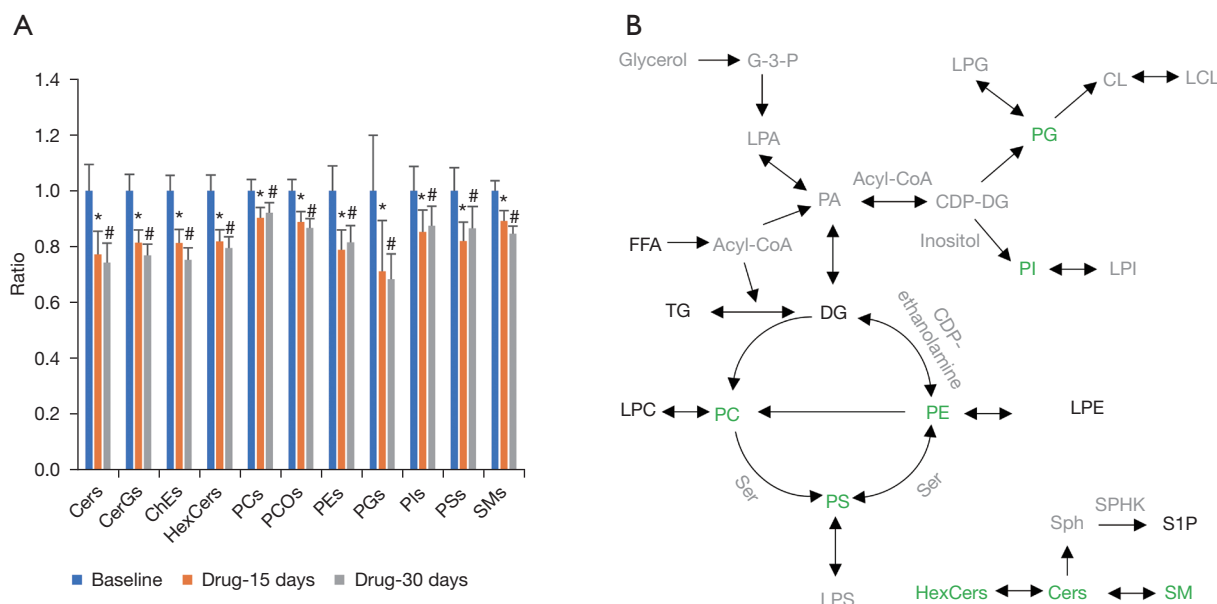


**Figure 3** Lipid changes during drug treatment. (A) Concentration ratios of significantly differential lipid (sub)classes among three groups; (B) lipid pathways. \*P<0.05 and FDR <0.05 for drug-15 days compared with baseline; #P<0.05 and FDR <0.05 for drug-30 days compared with baseline, green: significantly reduced during drug treatment, black: no statistical difference during drug treatment, light-grey: not detected. FDR, false discovery rate; Cer, ceramide; CerG, galactosylceramide; ChE, cholesteryl ester; CL, cardiolipin; CoQ, coenzyme Q; FFA, free fatty acid; DG, diacylglycerol; G-3-P, glycerol-3-phosphate; HexCer, hexosylceramide; LCL, lysocardiolipin; LPA, lysophosphatidic acid; LPC, lysophosphatidylcholine; LPE, lysophosphatidylethanolamine; LPS, lysophosphatidylserine; PA, phosphatidic acid; PC, phosphatidylcholine; PC O, ether bond-containing PC; PE, phosphatidylethanolamine; PG, phosphatidylglycerol; PI, phosphatidylinositol; PS, phosphatidylserine; SM, sphingomyelin; Sph, sphingosine; S1P, sphingosine-1-phosphate; TG, triacylglycerol; LPC O, ether bond-containing lysophosphatidylcholine.

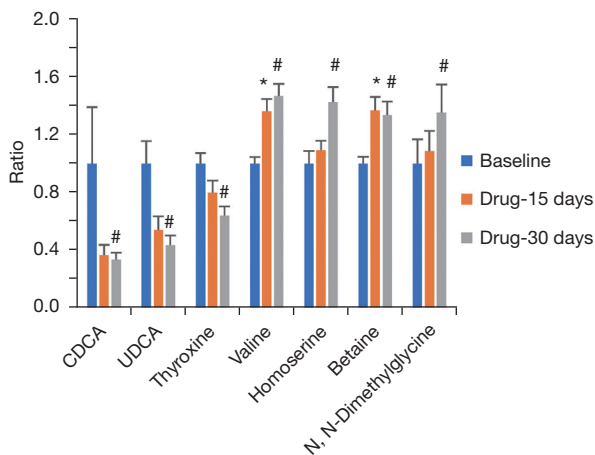


**Figure 4** Concentration ratios of significantly differential metabolites among the three groups the pathways of lipids. \*P<0.05 and FDR <0.05 for drug-15 days compared with baseline; #P<0.05 and FDR <0.05 for drug-30 days compared with baseline. FDR, false discovery rate; CDCA, chenodeoxycholic acid; UDCA, ursodeoxycholic acid.

We also investigated the pathways involved in bile acid metabolism (Figure 5B), and found the alternative pathway seemed to be more influenced by the drug treatment.

**Discussion**

Roxadustat can improve iron utilization by decreased ferritin, hepcidin and increased serum iron, transferrin; The principle is as follows: HIF-PHI can improve iron metabolism by upregulating molecules responsible for iron absorption and transport. HIF-1 may increase iron availability by upregulating transferrin, ceruloplasmin, and transferrin receptor 1, whereas HIF-2 regulates the expression of divalent metal transporter 1 (DMT1) and duodenal cytochrome b (Dcytb) (20,21). In addition, inflammation can inhibit renal EPO production and affects EPO function, and is an independent risk factor for ESA resistance; a study has confirmed that HIF-PHI may reduce the levels of inflammatory factors such as TNF- $\alpha$ , IL-1 $\beta$ ,

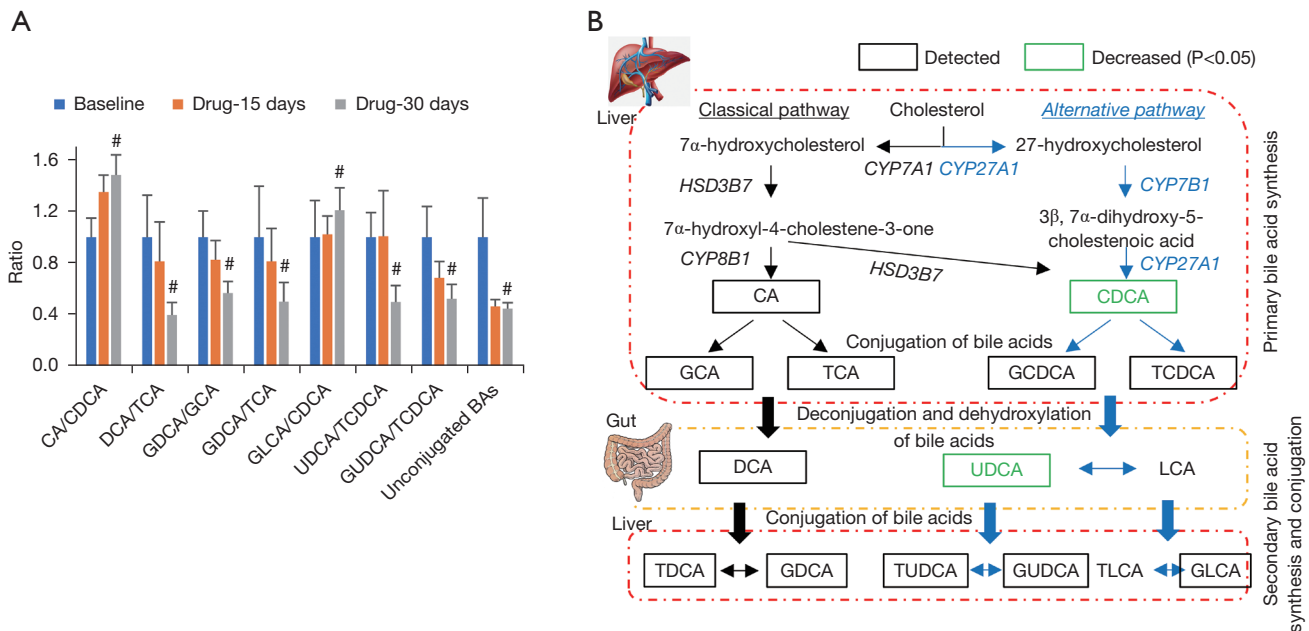


**Figure 5** Bile acids changes during drug treatment. (A) Concentration ratios of significantly differential bile acids among the three groups; (B) pathways of bile acids. \* $P < 0.05$  and  $FDR < 0.05$  for drug-15 days compared with baseline; <sup>#</sup> $P < 0.05$  and  $FDR < 0.05$  for drug-30 days compared with baseline.  $FDR$ , false discovery rate; CA, cholic acid; CDCA, chenodeoxycholic acid; DCA, deoxycholic acid; GCA, glycocholic acid; GCDCA, glycochenodeoxycholic acid; GDCA, glycodeoxycholic acid; GLCA, glycolithocholic acid; GUDCA, glyoursodeoxycholic acid; LCA, lithocholic acid; TCA, taurocholic acid; TCDC, taurochenodeoxycholic acid; TDC, tauroursodeoxycholic acid; TLCA, tauroolithocholic acid; TUDCA, tauroursodeoxycholic acid; UDCA, ursodeoxycholic acid.

IL-6; also HIF-PHI can promote adenosine gene expression and assist adenosine to exert anti-inflammatory effects (7); by increasing iron utilization and improving inflammatory status, roxadustat can stimulate endogenous erythropoietin production and thereby induce erythropoiesis.

In this study, we applied lipidomics and metabolomics platforms to investigate changes in serum metabolites during roxadustat treatment for up to 30 days in a cohort of 32 ESRD patients with ESA resistance. Lipidomics revealed Cers, HexCers, PCs, PEs, PIs, PSs, and SMs, as well as sphingolipid- and phospholipid-related pathways, were significantly reduced during roxadustat treatment. Previous research also showed PI and SM levels decreased in HeLa cells under hypoxic conditions compared with normal conditions (22), and activation of HIF-2 $\alpha$  by roxadustat could promote Cer catabolism in adipose tissue leading to reduced adipose and plasma Cer levels, to suppress atherosclerosis (23). In addition, Cers could promote the production of inflammatory factors such as interleukin (IL)-6 (24). Therefore, it is possible roxadustat might reduce Cer levels and improve the inflammatory state,

further correcting ESA resistance. Sphingosine-1-phosphate (S1P) is a potent signaling lipid secreted by red blood cells and platelets (25), and S1P levels have been shown to be significantly improved by stress-induced erythropoiesis (26). Although there were no significant changes in S1P levels among the groups in this study (data not shown), the increased trend during drug treatment might be related to erythropoiesis. Mammalian cell membranes are known to include phospholipids, such as PCs, PEs, PIs, PGs, and PSs, and in this study, most phospholipid classes were significantly decreased during drug treatment. Given red blood cell production is increased under hypoxic conditions (27) and by hypoxia-inducible factor (28), this could be a major reason for the decreased levels of phospholipids.

Metabolomics data indicated valine, homoserine, dimethylglycine, and betaine were increased after drug treatment, with all significantly increased after 30 days, and valine and betaine also significantly increased after 15 days compared with baseline. Branched-chain amino acids (BCAA) and aromatic amino acids were shown

to be increased in rats/mice exposed to acute hypoxia or hypoxic preconditioning (29,30). In glioblastoma, hypoxia upregulates mRNA and protein levels of the BCAA transporter LAT1 and the BCAA metabolic enzyme BCAT1 by HIF-1 $\alpha$  and HIF-2 $\alpha$  activation, and HIF-1 $\alpha$  directly binds to the hypoxia response element at the first intron of the human BCAT1 gene (31). Hence, we speculated that the increased levels of BCAAs were caused by HIF-1 $\alpha$  and HIF-2 $\alpha$  activation after roxadustat treatment.

The liver and gut are the main sites of bile acid metabolism, and bile acids are closely related to digestive absorption and disease development. Bile acid ratios could also indicate alterations in metabolism and enzymatic activities, and our results revealed CDCA and UDCA were significantly reduced after roxadustat treatment for 30 days. High levels of CDCA and UDCA have been reported to be cytotoxic and to promote cell death (32,33), and impaired mitochondrial function, as the cause of the cytotoxicity, was expressed via mitochondrial permeability transition (34). The ratios of certain bile acids could reflect enzymatic activities in the gut microbiome and liver (35). The CA/CDCA ratio increased significantly after drug treatment for 30 days compared with baseline, which might demonstrate a shift in bile acid synthesis from an alternative to the primary bile acid pathway in the liver. The ratios of secondary to primary bile acids, including DCA and TCA, were significantly decreased after roxadustat treatment for 30 days, suggesting changes in the activity of bacterial 7 $\alpha$ -dehydroxylases leading to reduced production of secondary bile acids. Unconjugated bile acids, including CA, CDCA, DCA, LCA, and UDCA, are potent endogenous signaling molecules of the farnesoid X receptor (35,36), which play important roles in controlling lipid and glucose metabolism, and in our study, unconjugated bile acids were significantly decreased after drug treatment for 30 days. Moreover, it was reported that more bile acids could be excreted into the feces if roxadustat was used to activate HIF-2 $\alpha$  in Hif2a<sup>fl/fl</sup>Apoe<sup>-/-</sup> mice (23), and we speculated this might be one reason for their decreased levels. Bile acids induce the macrophage TGR5 signaling pathway, leading to increased expression of the pro-inflammatory cytokines IL-1 $\beta$ , IL-6, and tumor necrosis factor (31). Although there is currently no direct evidence to support a relationship between bile acid metabolism and anemia, it is speculated decreased bile acid levels would reduce inflammation, with beneficial effects for the treatment of ESA resistance.

This study also had some limitations. We only investigated 96 samples from 32 participants and did

not validate the metabolomics and lipidomics results in additional samples. Furthermore, the proposed mechanism was not verified by other experiments, such as proteomics, cell lines, or animal models. Further studies are required to confirm these findings.

## Conclusions

In this study, we used lipidomics and metabolomics platforms to systemically investigate changes in the metabolome and lipidome caused by roxadustat in patients with ESRD and ESA resistance. The results revealed 30 days of drug treatment had substantial effects on the serum metabolome and lipidome. Lipidomics result revealed sphingolipids and phospholipids were significantly decreased during roxadustat treatment, suggesting the drug affected phospholipid and ceramide metabolism. Metabolomics results showed the CA/CDCA ratio was significantly increased, while bile acids showed an opposite change after roxadustat treatment. This may be associated with changes in bile acid metabolism caused by the gut microbiota. The current results indicate the combination of lipidomics and metabolomics could be used to investigate changes in metabolism caused by roxadustat in ESRD patients with ESA resistance. This may further our understanding of the detailed mechanism of roxadustat and help to prevent possible complications during its clinical use.

## Acknowledgments

*Funding:* This work was supported by the National Natural Science Foundation of China (Nos. 21874130, 22074144), the Key Foundation of Dalian City (No. 2019J11CY018), and Dalian Medical Science Research Project (No. 2011006). The Dalian Key Medical Specialty Dengfeng Project awarded grants (Nos. 2022ZZ231 and 2022ZZ243 to S Liu; No. 2022ZZ253 to Y Wu; No. 2022ZZ249 to L You; Nos. 2022ZZ235 and 2022ZZ247 to Z Wang; No. 2022ZZ237 to J Xiao; and No. 2022ZZ236 to S Zhang).

## Footnote

*Reporting Checklist:* The authors have completed the MDAR reporting checklist. Available at <https://atm.amegroups.com/article/view/10.21037/atm-22-4451/rc>

*Data Sharing Statement:* Available at <https://atm.amegroups.com/article/view/10.21037/atm-22-4451/dss>

*Conflicts of Interest:* All authors have completed the ICMJE uniform disclosure form (available at <https://atm.amegroups.com/article/view/10.21037/atm-22-4451/coif>). The authors have no conflicts of interest to declare.

*Ethical Statement:* The authors are accountable for all aspects of the work in ensuring that questions related to the accuracy or integrity of any part of the work are appropriately investigated and resolved. The study was approved by the Institutional Medical Ethics Committee of Dalian Municipal Central Hospital (No. 2020-044-08), and all participants provided written informed consent after reviewing the study plan. The study was conducted in accordance with the Declaration of Helsinki (as revised in 2013).

*Open Access Statement:* This is an Open Access article distributed in accordance with the Creative Commons Attribution-NonCommercial-NoDerivs 4.0 International License (CC BY-NC-ND 4.0), which permits the non-commercial replication and distribution of the article with the strict proviso that no changes or edits are made and the original work is properly cited (including links to both the formal publication through the relevant DOI and the license). See: <https://creativecommons.org/licenses/by-nc-nd/4.0/>.

## References

1. Fujimoto D, Adachi M, Miyasato Y, et al. Efficacy of continuous erythropoietin receptor activator for end-stage renal disease patients with renal anemia before and after peritoneal dialysis initiation. *Clin Exp Nephrol* 2021;25:191-9.
2. Mikhail A, Brown C, Williams JA, et al. Renal association clinical practice guideline on Anaemia of Chronic Kidney Disease. *BMC Nephrol* 2017;18:345.
3. Zuo L, Wang M, Hou F, et al. Anemia Management in the China Dialysis Outcomes and Practice Patterns Study. *Blood Purif* 2016;42:33-43.
4. Pan S, Zhao DL, Li P, et al. Relationships among the Dosage of Erythropoiesis-Stimulating Agents, Erythropoietin Resistance Index, and Mortality in Maintenance Hemodialysis Patients. *Blood Purif* 2022;51:171-81.
5. IV. NKF-K/DOQI Clinical Practice Guidelines for Anemia of Chronic Kidney Disease: update 2000. *Am J Kidney Dis* 2001;37:S182-238.
6. Drüeke T. Hyporesponsiveness to recombinant human erythropoietin. *Nephrol Dial Transplant* 2001;16 Suppl 7:25-8.
7. Yan Z, Xu G. A Novel Choice to Correct Inflammation-Induced Anemia in CKD: Oral Hypoxia-Inducible Factor Prolyl Hydroxylase Inhibitor Roxadustat. *Front Med (Lausanne)* 2020;7:393.
8. Weir MR. Managing Anemia across the Stages of Kidney Disease in Those Hyporesponsive to Erythropoiesis-Stimulating Agents. *Am J Nephrol* 2021;52:450-66.
9. Chen N, Hao C, Liu BC, et al. Roxadustat Treatment for Anemia in Patients Undergoing Long-Term Dialysis. *N Engl J Med* 2019;381:1011-22.
10. Afshinnia F, Rajendiran TM, Karnovsky A, et al. Lipidomic Signature of Progression of Chronic Kidney Disease in the Chronic Renal Insufficiency Cohort. *Kidney Int Rep* 2016;1:256-68.
11. Chen H, Cao G, Chen DQ, et al. Metabolomics insights into activated redox signaling and lipid metabolism dysfunction in chronic kidney disease progression. *Redox Biol* 2016;10:168-78.
12. Dou F, Miao H, Wang JW, et al. An Integrated Lipidomics and Phenotype Study Reveals Protective Effect and Biochemical Mechanism of Traditionally Used *Alisma orientale* Juzepzuk in Chronic Kidney Disease. *Front Pharmacol* 2018;9:53.
13. Liu X, Zhang B, Huang S, et al. Metabolomics Analysis Reveals the Protection Mechanism of Huangqi-Danshen Decoction on Adenine-Induced Chronic Kidney Disease in Rats. *Front Pharmacol* 2019;10:992.
14. Lee T, Clavel T, Smirnov K, et al. Oral versus intravenous iron replacement therapy distinctly alters the gut microbiota and metabolome in patients with IBD. *Gut* 2017;66:863-71.
15. Zhang ZH, He JQ, Zhao YY, et al. Asiatic acid prevents renal fibrosis in UO rats via promoting the production of 15d-PGJ2, an endogenous ligand of PPAR- $\gamma$ . *Acta Pharmacol Sin* 2020;41:373-82.
16. Thome T, Kumar RA, Burke SK, et al. Impaired muscle mitochondrial energetics is associated with uremic metabolite accumulation in chronic kidney disease. *JCI Insight* 2020;6:139826.
17. He H, An F, Huang Q, et al. Metabolic effect of AOS-iron in rats with iron deficiency anemia using LC-MS/MS based metabolomics. *Food Res Int* 2020;130:108913.
18. Ahmed A, Slater R, Lewis S, et al. Using Volatile Organic Compounds to Investigate the Effect of Oral Iron Supplementation on the Human Intestinal Metabolome. *Molecules* 2020;25:5113.
19. Locatelli F, Aljama P, Bárány P, et al. Revised European

- best practice guidelines for the management of anaemia in patients with chronic renal failure. *Nephrol Dial Transplant* 2004;19 Suppl 2:ii1-47.
20. Sugahara M, Tanaka T, Nangaku M. Future perspectives of anemia management in chronic kidney disease using hypoxia-inducible factor-prolyl hydroxylase inhibitors. *Pharmacol Therapeut* 2022;239:108272.
  21. Hou YP, Wang C, Mao XY, et al. Roxadustat regulates iron metabolism in dialysis-dependent and non-dialysis-dependent chronic kidney disease patients: A meta-analysis. *J Formos Med Assoc* 2022. [Epub ahead of print]. doi: 10.1016/j.jfma.2022.06.008.
  22. Yu Y, Vidalino L, Anesi A, et al. A lipidomics investigation of the induced hypoxia stress on HeLa cells by using MS and NMR techniques. *Mol Biosyst* 2014;10:878-90.
  23. Zhang X, Zhang Y, Wang P, et al. Adipocyte Hypoxia-Inducible Factor 2 $\alpha$  Suppresses Atherosclerosis by Promoting Adipose Ceramide Catabolism. *Cell Metab* 2019;30:937-51.e5.
  24. Chaurasia B, Summers SA. Ceramides - Lipotoxic Inducers of Metabolic Disorders. *Trends Endocrinol Metab* 2015;26:538-50.
  25. Gazit SL, Mariko B, Thérond P, et al. Platelet and Erythrocyte Sources of S1P Are Redundant for Vascular Development and Homeostasis, but Both Rendered Essential After Plasma S1P Depletion in Anaphylactic Shock. *Circ Res* 2016;119:e110-26.
  26. Vu TM, Ishizu AN, Foo JC, et al. Mfsd2b is essential for the sphingosine-1-phosphate export in erythrocytes and platelets. *Nature* 2017;550:524-8.
  27. Haase VH. HIF-prolyl hydroxylases as therapeutic targets in erythropoiesis and iron metabolism. *Hemodial Int* 2017;21 Suppl 1:S110-24.
  28. Fandrey J. Oxygen-dependent and tissue-specific regulation of erythropoietin gene expression. *Am J PhysiolRegulIntegr Comp Physiol* 2004;286:R977-88.
  29. Muratsubaki H, Yamaki A. Profile of plasma amino Acid levels in rats exposed to acute hypoxic hypoxia. *Indian J Clin Biochem* 2011;26:416-9.
  30. Liu J, Zhan G, Chen D, et al. UPLC-QTOFMS-based metabolomic analysis of the serum of hypoxic preconditioning mice. *Mol Med Rep* 2017;16:6828-36.
  31. Zhang B, Chen Y, Shi X, et al. Regulation of branched-chain amino acid metabolism by hypoxia-inducible factor in glioblastoma. *Cell Mol Life Sci* 2021;78:195-206.
  32. Ignacio Barrasa J, Olmo N, Pérez-Ramos P, et al. Deoxycholic and chenodeoxycholic bile acids induce apoptosis via oxidative stress in human colon adenocarcinoma cells. *Apoptosis* 2011;16:1054-67.
  33. Rolo AP, Palmeira CM, Wallace KB. Mitochondrially mediated synergistic cell killing by bile acids. *BiochimBiophys Acta* 2003;1637:127-32.
  34. MahmoudianDehkordi S, Arnold M, Nho K, et al. Altered bile acid profile associates with cognitive impairment in Alzheimer's disease-An emerging role for gut microbiome. *Alzheimers Dement* 2019;15:76-92.
  35. Lefebvre P, Cariou B, Lien F, et al. Role of bile acids and bile acid receptors in metabolic regulation. *Physiol Rev* 2009;89:147-91.
  36. Claudel T, Staels B, Kuipers F. The Farnesoid X receptor: a molecular link between bile acid and lipid and glucose metabolism. *ArteriosclerThrombVasc Biol* 2005;25:2020-30.
- (English Language Editor: B. Draper)

**Cite this article as:** Wang L, Wu Y, Li Y, You L, Liu X, Wang Z, Xiao J, Zhang S, Xu T, Wang X, Li Q, Hu C, Xu G, Liu S. Effect of roxadustat on serum metabolome and lipidome in patients with end-stage renal disease and erythropoiesis-stimulating agent resistance. *Ann Transl Med* 2022;10(19):1069. doi: 10.21037/atm-22-4451

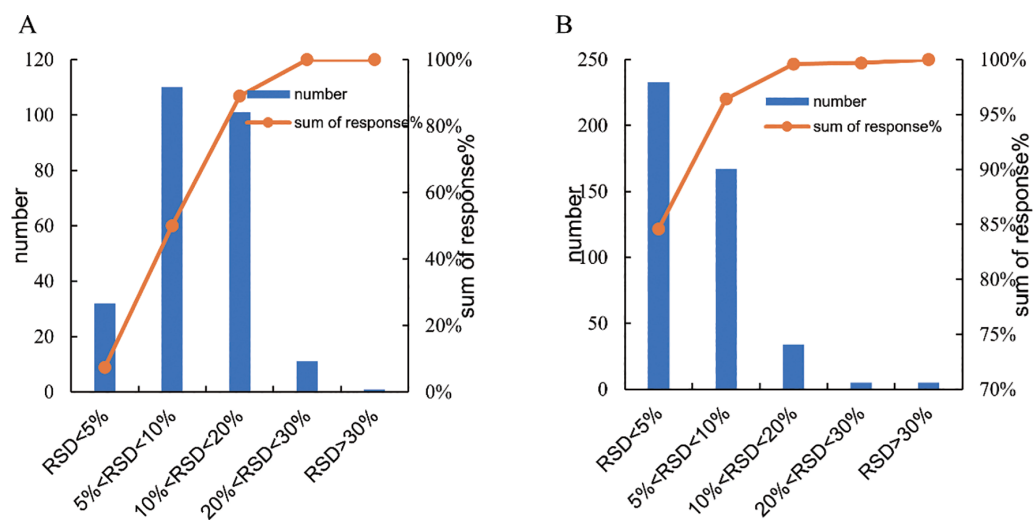


**Figure S1** CV distribution of all detected metabolites and lipids in 11 QCs. Number %, percentage of number of lipids within a defined range of CV value. Sum of response %, percentage of total response of lipids below a special criteria of CV value. (A) Metabolomics; (B) lipidomics. CV, coefficient of variation; QCs, quality control samples; RSD, relative standard deviation.